PAPER

A 2-D Amplifying Array Using Multi-Ported Aperture-Coupled Patch Antennas

Tan-Hsiung HO[†], **Wei-Jen CHEN**[†], *and* **Shyh-Jong CHUNG**[†a)], ***Members***

SUMMARY This paper proposes a new circuit-fed 2-D amplifying array architecture using the multi-ported aperture-coupled patch antennas. The power distribution achieved by this array is formed by stacking three kinds of basic cells repeatedly. Each cell, which serves as a radiator and also a power relay, has a multi-ported patch antenna and one or two amplifiers. The signal transmission coefficient of the cell from the input port to the output port is designed with a power level of 0 dB and a phase of 360°. An X-band 4 × 3 element array with uniform amplitude distribution is demonstrated. The measured results, such as the antenna gain and the radiation patterns, agree very well with the predicted ones, due to the precision design of the basic cells. The measured gain of the antenna array is 27.7 dBi_A at the frequency of 10.4 GHz on the H-plane, with a half-power beamwidth of 14° in the H-plane and 16° in the E-plane.

key words: *amplifying array, active antenna, multi-ported patch antenna, high gain antenna*

1. Introduction

Microstrip antenna arrays are popular for various applications due to the benefits of compact size and high circuit integrality. The microstrip patch antenna is particularly compatible with modern monolithic integrated circuit (MIC) technology, and solid-state devices have been used to combine several component functions at the terminals of the patch antenna. The integrated antennas can reduce the size, weight, and cost of many transmitting and receiving systems. These active integrated antennas are ideal for spatial and quasi-optical power combination for high power applications. The planar architecture, because of its low profile and weight, is attractive for such applications as airborne radar and satellite communications [1]–[5]. Among these studies, a conventional parallel-fed network is commonly used to distribute the input power to each antenna element, and a solid-state amplifier can be embedded in the front of each element to amplify the distributed power. This design is simple but lots of power dividers are required for a large array. Furthermore, there is a high transmission loss for a huge array due to the losses from the extremely long feed lines, and eventually a gain saturation effect would be occurred when the array size is large enough. In [1], a distributive amplify array is introduced using the horn antenna. Which overcomes the problem caused by the power distribution network but it costs large space. Another one-dimensional series-fed amplifying antenna array using a patch antenna coupler, which has the advantages of easy bias and no power divider required, is proposed [6]. However, this series-fed one is difficult to be extended to two dimensions on the same circuit layer since there is no enough area to contain the extended active and passive elements.

In this paper, a new 2-D amplifying antenna array using multi-ported aperture coupled patch antennas is proposed. Figure 1 illustrates the architecture of the array, which is composed of antenna elements, couplers, and amplifiers. For the entire circuit layout, since the antennas and circuits have to be fabricated on different substrate layers with an orderly arrangement, the aperture-coupled structure is adopted [7]. Although the architecture of the array seems very complicated, it is methodically constructed by three simple and basic cells, which are one-, two-, and three-ported. The one-ported cell, composed of a traditional one-port aperture-coupled antenna with a feed microstrip line, is used for terminating each row of the array. The other two basic cells integrate two elements, i.e., an amplifier and a radiating element with one or two couplers. Assembling the three basic cells and then connecting each other in sequence can implement an M×N two-dimensional array with unlimited extension, as illustrated in Fig. 2. When the power is fed to the first element through the array input port, with most of the power radiated by the first three-port antenna, part of the power is spared by the aperture couplers to the vicinity. The coupled power is amplified by a FET amplifier and then fed to the next antenna element. One of the output ports from the three-ported cell can be connected to another three-

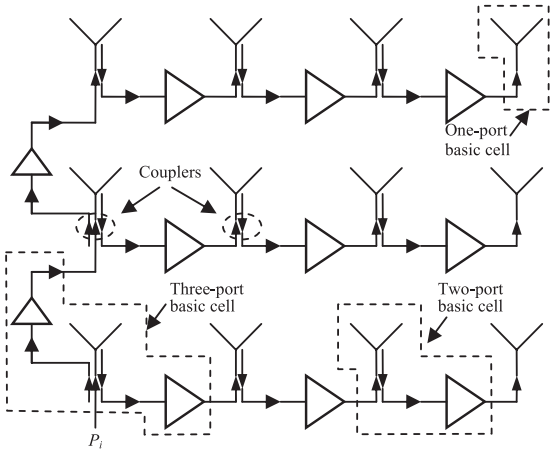

Fig. 1 Diagram of the proposed 2-D amplifying array.

Manuscript received September 10, 2008.
Manuscript revised February 17, 2009.

[†]The authors are with the Department of Communication Engineering, National Chiao Tung University, Taiwan.
a) E-mail: sjchung@cm.nctu.edu.tw

DOI: 10.1587/transcom.E92.B.2461

ported cell to create a new branch while the other one should be connected to a two-ported cell to start the power distribution on a row. The two-ported cell is similar to the three-ported cell but only one output port, which radiates most of the input power and amplifies the remnant power. Eventually, the powers are terminated at the one-ported cell at the end of each row. To form an array with a uniform power distribution, the first step is to design the two- and three-ported basic cells with transmission gain and phase delay equal to 0 dB and multiple of 360° respectively. The transmission gain and phase can be achieved by carefully tuning the power gain provided by the amplifier and the lengths of the microstrip lines connecting to the adjacent antennas. After that cascade the well designed cells in sequence (as shown in Fig. 2), a 2-D amplifying array with any size can achieve effortlessly.

Based on this excitation technique, a 4 × 3 two-dimensional amplifying array is formed and demonstrated. Compared with the conventional amplifying array, the proposed one is more compact and no bulky power-divider network is needed. For a large-sized amplifying array, the mutual coupling between antenna elements and feed circuits may induce the spurious radiation, which degrades the sidelobe levels and increases the cross polarization. By adopting the aperture-coupled structure, the patch antennas are completely shielded from the feeds, so the effect can be eliminated. In addition, even through the array size is large, there is no gain saturation effect resulted from the extremely long feed line losses. Moreover, by using the modular approach described above, a beam-shaped and high gain amplifying array can be constructed quickly after stacking the building blocks.

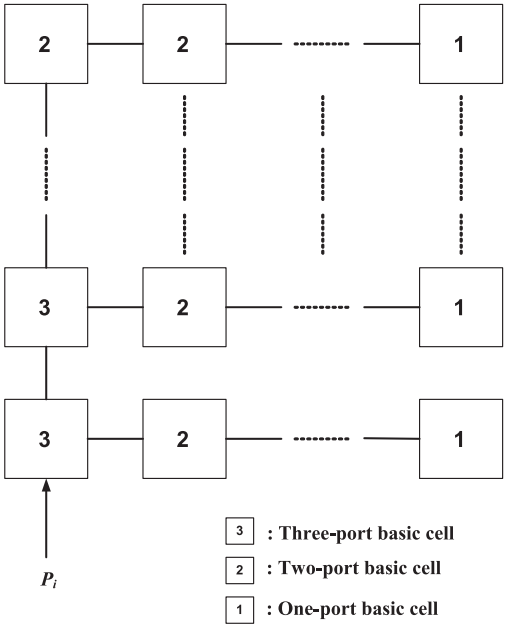

Fig. 2 Architecture of the proposed 2-D amplifying array with an arbitrary extension constructed by stacking three basic cells.

2. Multi-Ported Patch Antennas

The 2D amplifying array is formed by three kinds of basic cells. Within each basic cell, the radiating element is co-designed with each cell to radiate some power to the space. In this paper, an aperture-coupled patch antenna is proposed because of the benefits of lower circuit radiation and easier circuit placement and routing. The antenna patches are built on a 31-mil Duroid 5870 (ε_r = 2.33) substrate, where the copper on the bottom plane is completely removed, and the microstrip circuits are formed on a 20-mil Duroid 5880 (ε_r = 2.2) substrate. In the following, the design and implementation of each component is to be depicted.

2.1 Two-Port Aperture-Coupled Microstrip Antenna

The sketch of the two-port antenna is shown in Fig. 3(a). The patch antenna and microstrip lines are fabricated on the different substrates separated by a common ground. Within this layout, there are two slots on the ground. The slot in the center feeds the power into the antenna while the other one placed under the edge of the patch couples a little power

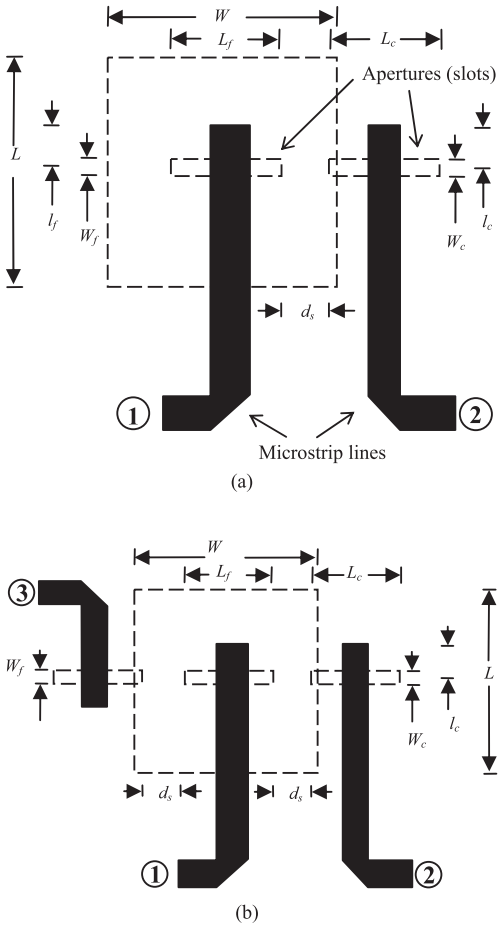

Fig. 3 Configurations of (a) the 2-ported and (b) 3-ported aperture coupled patch antennas.

from the patch and deliver it to the following cells. The feeding port is placed below the center of the patch for maximal power coupling. A conventional one-port aperture-coupled antenna can be designed first to verify that the coupling port weakly influences the performance of the patch and feed line [8]. 50-ohm microstrip lines with the width w_{50} (=1.57 mm) are used to feed the antenna and extract slightly the power from the patch through the feeding and coupling apertures. The length and width of the coupling slot will influence the center frequency and bandwidth slightly. The slots are designed to be with the same length of 4.5 mm, which is approximate to a quarter of the wavelength within the substrate, and width of 0.58 mm. The location of the coupling slot on the ground plane may influence the resonant condition and thus change the resonant frequency of antenna. The coupling slot was placed with a little area overlap under the patch (the space between two slots d_s were fixed to be 1.05 mm) to minimize the influence by additional slot. Both the microstrip lines symmetrically cross over the center of the apertures with matching stubs of length l_f and l_c. A full-wave EM simulator IE3D [9] is adopted for simulation of this structure. The designed length (L) and width (W) of the patch antenna with an aperture coupler, for an operating frequency at 10 GHz, are 8 and 7.5 mm respectively. Although placing an extra coupling slot on the ground plane would influence the resonant condition and thus change the resonant frequency of antenna, this effect is small (since the coupling is weak) and can be simply compensated by finely tuning the lengths of the patch and feed matching stubs. Adjusting the stub length of the feeding port and the length of the patch can dominate the input matching and the resonant frequency, while varying the stub length of the coupling port can control the level of the coupling energy. The designed lengths of the stubs of the feeding and coupling ports are 1.8 and 1.77 mm, respectively.

The fabricated two-port antenna shows a resonant frequency at 10.03 GHz with a 10 dB return-loss bandwidth of 4.3%. The measured coupling coefficient (|S21|) reaches a maximum of −8.5 dB around the resonant frequency. For verification, the measured result is obtained using the TRL calibration technique. The antenna gain is 6.2 dBi at 10 GHz, which is quiet similar to the simulated result (6.4 dBi). The 3-dB beamwidth of the E-plane is 78.5°, and that of H-plane is 83.2°, as shown in Fig. 4(a).

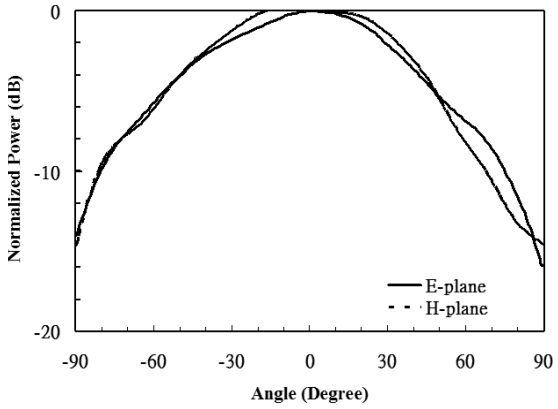

(a)

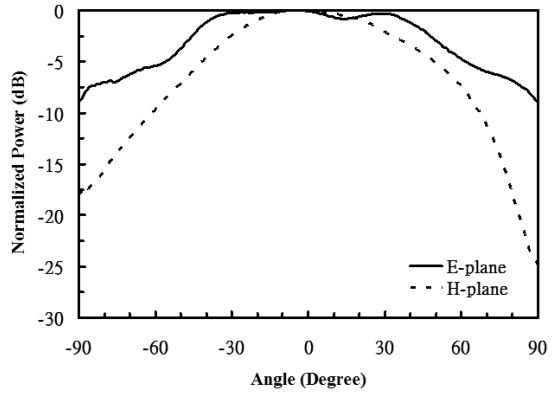

(b)

Fig. 4 Measured E- and H-plane radiation patterns of (a) the 2-ported and (b) 3-ported aperture coupled patch antennas.

2.2 Three-Port Aperture-Coupled Microstrip Antenna

The geometry of the three-port aperture-coupled antenna is shown in Fig. 3(b). Compared with the traditional one-port aperture-coupled antenna, the three-port one has two extra slots on the ground plane, which are located under the left and right non-radiation edges of the patch, respectively. For this three-port antenna with dual aperture couplers, the magnitude of the coupling coefficient of port-2 is identical to that of port-3 due to the symmetry of the two coupling slots. However, the phase difference between these two coupling coefficients is out-of-phase since the two coupled microstrip lines are placed upside-down. In contrast to the two-port antenna, although the existence of the extra slot would influence the matching and coupling coefficients of the antenna, repeatedly, the effect is small and can be compensated by carefully tuning the matching stubs of the feeding and coupling ports. After tuning, the stub lengths of the feeding and coupling ports are 2.06 and 2.34 mm, respectively. The fabricated prototype presents a resonant frequency at 10.03 GHz and a 10-dB return-loss bandwidth of 4.5%. The measured coupling coefficients (|S21| and |S31|) of the three-port antenna are quite the same as each other with a level of −9 dB around the resonant frequency, and the difference between the measured phase delays (∠S21 and ∠S31) is approximately 180°. The antenna gain is 5.91 dBi measured at 10 GHz, which is a little lower than that of the two-port antenna. The gain reduction may be caused due to the power coupling resulted from the extra aperture coupler. The 3-dB beamwidths of the E- and H- plane are 98.1° and 70.2°, respectively, as shown in Fig. 4(b).

The antenna gain of both two- and three-ported aperture coupled antenna are a little lower than that of the conventional one. The gain reduction is caused due to the power coupling resulted from the extra aperture coupler. The purpose of designing the two- and three-port aperture-coupled antennas is to control power coupling from the input port to

the coupling port. Different levels of the power coupling can be achieved by varying the length (l_c) of the coupled line so as to make the basic cells, which are composed of the antenna and amplifier to meet the requirement of the transducer gain and phase delay.

3. Design of Unit Cells

As shown in Fig. 1, the proposed amplifying array is constructed using three kinds of basic cells, which are three-, two-, and single-port cells. The three-port cell is a three-port sub-circuit which has one input and two output ports. The three-port cell acts as a branch knot which is placed near the feed point of the array to generate a new branch. A portion of the power radiates in this element and the remaining portions are delivered to the output port after amplifying. The two-port cell acts as a signal relay to extend a branch. Similar to the three-port cell, the two-port cell radiates some power to space and passes the remains to the following cells after amplifying. The transmission gain and phase delay through the three- and two-port cells should be critically designed to be unitary and a multiple of 360°.

Figure 5 depicts the geometry of the two- and three-port basic cells. Each cell combines the FET amplifier and relative multi-ported antennas. The FET amplifier is designed with the device NE32584C at the bias condition of V_{DS} = 2 V and I_D = 20 mA. The measured gain has a level of 9.5 dB at 10 GHz with approximately 0.5-dB gain flatness from 9.24 GHz to 10.56 GHz. The return loss at the center frequency is better than −35 dB. The measured phase delay with additional 1-mm extension at both input and output ports is 69°, which shows a good agreement with the simulation one.

To meet the requirement of a uniform power distribution, the stub length at the coupling port of the aperture-coupled antenna could be adjusted to obtain a suitable coupling level. For broadside radiation, the signal phases at the feed points of all the patch antennas should be the same. This is accomplished by designing the lengths of the feed lines connecting to adjacent antennas so that the signal phase delay would be equal to a multiple of 360°.

Figure 6 and Fig. 7 give the measured transmission gain of the two- and three-ported basic cells, respectively. The phase delay is contributed by the antenna, the FET amplifier, and two extra sections of microstrip lines (before and after the amplifier). The phase delays through the first two components are fixed from the above design, while the two extra

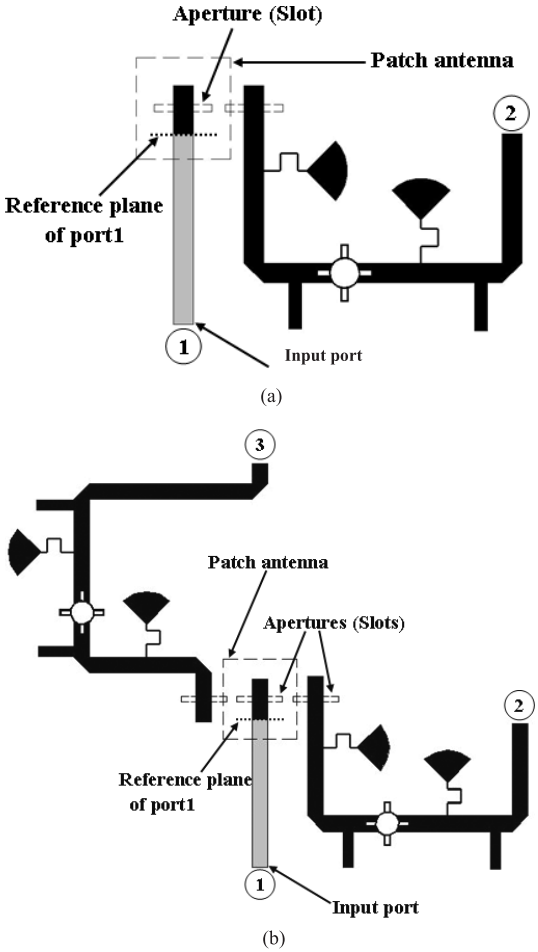

Fig. 5 Geometry of the (a) 2-ported and (b) 3-ported basic cells.

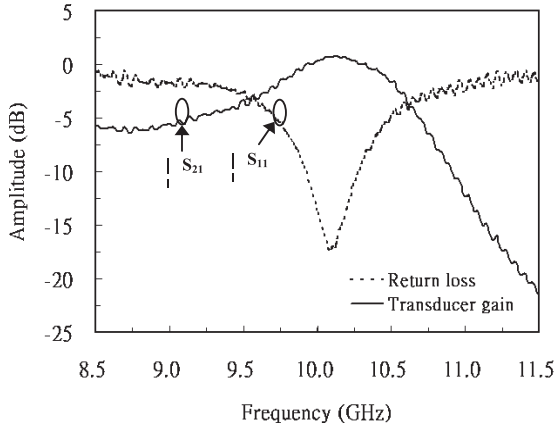

Fig. 6 The measured transmission gain of the 2-ported basic cell.

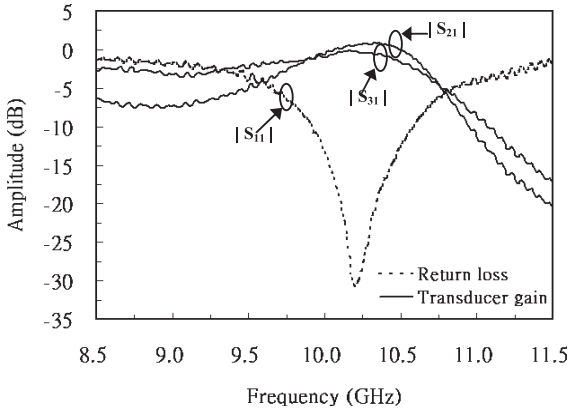

Fig. 7 The measured transmission gain of the 3-ported basic cell.

microstrip lines can be tuned to satisfy the phase requirement by adjusting the lengths. Both the basic cells have a transmission gain of 0-dB with a maximum error of 0.7 dB around the resonant frequency. The measured phase delay ($\angle$S21) of the two-port element, after incorporating the effect of the extended input feed line, corresponds to the phase difference of $-8.8°$ between the feed points of the first and second antenna elements. Also, the relative phase delays ($\angle$S21 and $\angle$S31) of the three-port element are $-2.4°$ and $2.5°$ around 10 GHz, which correspond to the phase differences from input port to the second and third ports, respectively.

4. 2-D Amplifying Array

Cascading and connecting the basic cells designed above can construct the entire amplifying antenna array. The two-dimensional array is implemented with 4×3 antenna elements. These elements are equally spaced along x- and y-axis with a distance (d) of 26.25 mm, which is 0.91 wavelength at 10.4 GHz. Figure 8 shows the top-view and bottom-view photos of the fabricated array. The antennas are placed on the top side while other components such as the amplifiers, transmission lines, and the bias network are placed on the bottom side. The return loss, antenna gain, and the radiation patterns are measured. Figure 9 illustrates the measurement results for the return loss, which is below 10 dB in the frequency range from 10 to 10.7 GHz and shows a resonant frequency of 10.33 GHz. The center frequency shift is mainly contributed by the coupling of adjacent elements.

The gain and radiation patterns of the amplifying array are measured using an X-band standard horn antenna with a gain of 15.9 dBi at 10.4 GHz [10]. The receiving horn connected to a power meter is placed at a distance of 220 cm, which is in the far-field zone of the array. The arrangement for the measurement is exhibited in Fig. 10. Since the two-dimensional array is formed along the E-plane and H-plane of the antenna element, both the E-plane and H-plane patterns are concerned and measured. Figure 11 depicts the results. For comparison, the calculated radiation patterns are also shown, which are obtained by multiplying the array factor through the element pattern of a single patch antenna [11], [12]:

$$|E_E(\theta)| = \left|\frac{1}{3}E_{nE}(\theta)\left(1 + e^{jkd\sin\theta} + e^{j2kd\sin\theta}\right)\right| \quad \text{for E-plane} \tag{1}$$

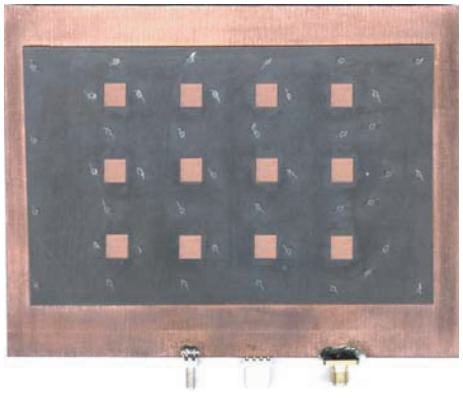

(a)

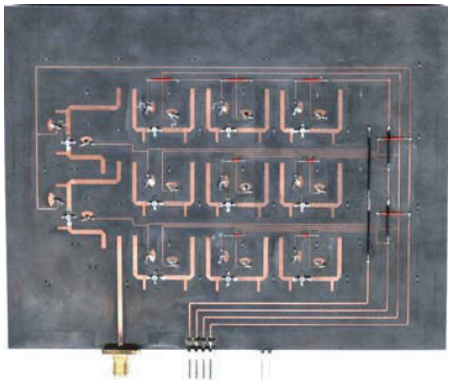

(b)

Fig. 8 (a) The top-view and (b) bottom-view of the fabricated amplifying array.

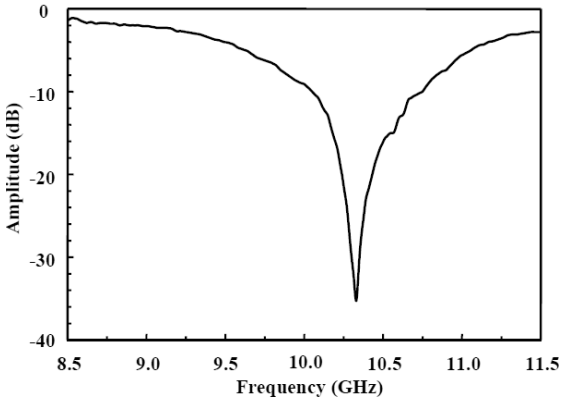

Fig. 9 Measured return loss as a function of the frequency for the fabricated 2-D amplifying array.

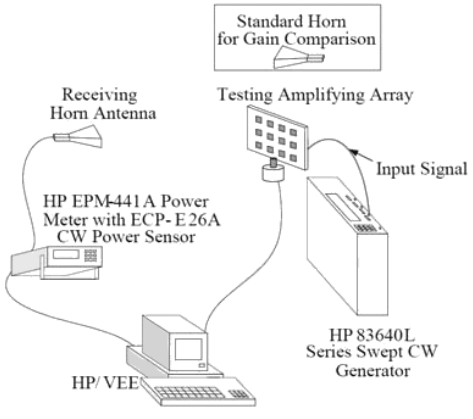

Fig. 10 Arrangement for measuring the antenna gain and radiation patterns of the amplifying array.

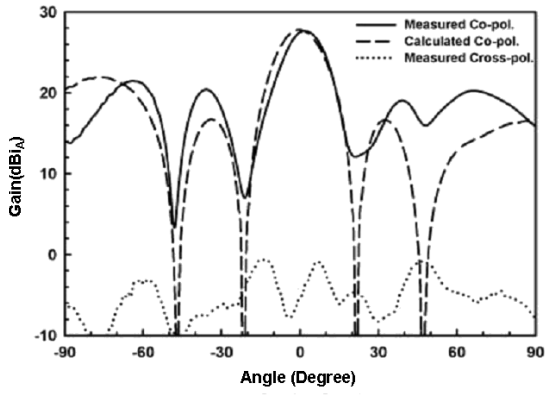

(a)

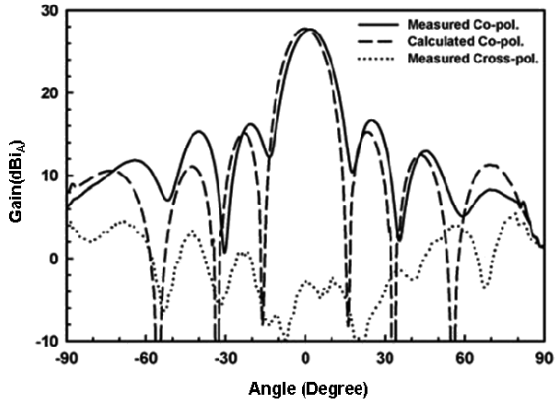

(b)

Fig. 11 (a) E-plane and (b) H-plane radiation patterns of the 4 × 3 2-D amplifying array. V_{DS} = 2 V, I_D = 20 mA, f = 10.4 GHz.

$$|E_H(\theta)| = \left|\frac{1}{4}E_{nH}(\theta)\left(1+e^{jkd\sin\theta}+e^{j2kd\sin\theta}+e^{j3kd\sin\theta}\right)\right| \quad \text{for H-plane} \tag{2}$$

where $E_{nE}(\theta)$ and $E_{nH}(\theta)$ denote the normalized E- and H-plane patterns of single patch antenna, respectively, while $E_E(\theta)$ and $E_H(\theta)$ express the normalized radiation patterns of the antenna array. For the authenticity of pattern prediction, the patterns of $E_{nE}(\theta)$ and $E_{nH}(\theta)$ are substituted by the measured patterns of the two- and three-port antennas instead of the calculated ones.

The measured E-plane pattern of the array in Fig. 11(a) possess a 3-dB beamwidth of 16° and a first side-lobe level of −8 dB, which are close to the calculation ones (18° and −12 dB, respectively). The measured H-plane pattern in Fig. 11(b) has a beamwidth of 14° and a side-lobe level of −11 dB, also in the good agreements with the predicted ones (14° and −12 dB). The maximum gain measured is 27.7 dBi$_A$ on the H-plane at 10.4 GHz with 2° shift from the broadside direction. This value is very close to the calculated array gain 27.5 dBi$_A$, which is 21.6 dB higher than the gain of a single three-port patch antenna. The main beam shift on both E- and H- plane is because of the transmission phase delay through the three- and two-ported cells respectively. The side-lobe level is higher than the predicted one because of the divergence of amplitude at each element. Since the radiation pattern of each cell is not exactly the same, which result in the asymmetrical pattern in both the calculated and measured one. The cross-polarization levels of the measured E- and H-plane are 25 dB lower than the co-polarization levels.

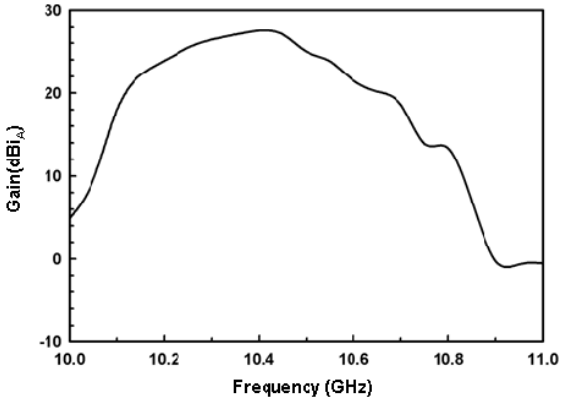

Fig. 12 The antenna gain of the 2-D amplifying array measured at broadside as a function of frequency.

Compare to a conventional array without amplifying that gain is 10 log(n), the gain of proposed one is 20 log(n) because of the power at each radiating element is equal to the input of array.

Figure 12 presents the measured frequency response of the array gain at broadside direction. The gain reaches to a maximum around 10.4 GHz and decreases as the operating frequency shifts from the center frequency because the phase delay of the transmission lines between adjacent antenna elements is designed to be a multiple of 360° at 10.4 GHz. The waves radiated from antenna elements are in-phase and then accumulate together at a broadside point in the far field only at this frequency. At other frequencies, each succeeding element has a phase delay relative to the preceding one, so that the beam is steered as the operating frequency varies, which results in the reduction of broadside gain.

5. Conclusion

An X-band 4 × 3 circuit-fed two-dimensional amplifying array using the multi-ported aperture-coupled patch antenna is proposed and demonstrated. This array is constructed using three kinds of basic cells and stacking the cells in sequence without designing the feeding network. With this design, as the array size increases, there is no gain saturation effect resulted from the extremely long feed line losses. The return loss of the demonstrated one has a center frequency at 10.33 GHz and 6.8% 10-dB return-loss bandwidth. The peak gain of the amplifying array comes to 27.7 dBi$_A$ in the H-plane with a 2° shift from the broadside direction at 10.4 GHz, which is very close to the predicted one of 27.5 dBi$_A$, The E-plane patterns of the array possess a half-power beamwidth of 16° and a first side-lobe level

of −8 dB, while the H-plane pattern possesses those of 14° and −11 dB, respectively. All agrees very well with the calculated ones. The proposed antenna array architecture has the advantages of high transmitting power, no power divider needed, compact, easy bias/construction by stacking the basic cells, and better array efficiency. The amplifying array architecture can readily utilized in many radar and point to point communication applications.

References

[1] H.J. Song and M.E. Bialkowski, "Transmit array of transistor amplifiers illuminated by a patch array in the reactive near-field region," IEEE Trans. Microw. Theory Tech., vol.49, issue 10, no.4, pp.470–475, March 2001.
[2] J.A. Navarro and K. Chang, Integrated Active Antennas and Spatial Power Combining, John Wiley, New York, 1996.
[3] R.A. York and Z.B. Popovic, Active and Quasi-Optical Arrays for Solid-State Power Combining, John Wiley, New York, 1997.
[4] A. Mortazawi, T. Itoh, and J. Harvey, eds., Active Antennas and Quasi-Optical Arrays, IEEE Press, Piscataway, NJ, 1998.
[5] M. Belaid, J.-J. Laurin, and K. Wu, "Integrated active antenna array using unidirectional dielectric radiators," IEEE Trans. Microw. Theory Tech., vol.48, issue 5, no.12, pp.1628–1634, Oct. 2000.
[6] C.-H. Tsai, Y.-C. Yang, S.-J. Chung, and K. Chang, "A novel amplifying antenna array using patch-antenna couplers — Design and measurement," IEEE Trans. Microw. Theory Tech., vol.50, issue 10, no.4, pp.1919–1926, Aug. 2002.
[7] D.M. Pozar, "Microstrip antenna aperture-coupled of a rectangular microstrip resonator," Electron. Lett., vol.22, pp.554–556, May 1986.
[8] W.J. Tseng and S.J. Chung, "Analysis and application of a two-port aperture-coupled microstrip antenna," IEEE Trans. Microw. Theory Tech., vol.46, issue 5, no.12, pp.530–535, May 1998.
[9] IE3D Manual, Zeland Software Inc, CA, USA.
[10] J.W. Cripin and K.M. Siegel, eds., Method of Radar Cross-Section Analysis, Academic Press, New York and London, 1968.
[11] W.L. Stutzman and G.A. Thiele, Antenna Theory and Design 2nd ed., John Wiley & Sons, New York, 1997.
[12] R.A. Sainati, CAD of Microstrip Antennas for Wireless Applications, Artech House, Boston and London, 1996.

Tan-Hsiung Ho received the B.S. and M.S. degrees in Communication Engineering from National Chao-Tung University in 2002 and 2003, respectively. Since 2003, he stays in Advanced Microwave Technology Laboratory, Communication Engineering Dept. National Chiao-Tung University to study antennas, millimeter-wave circuit, and automotive radar system. He is now working for the Chaolong-Technology Corp. Taiwan, to develop the automotive digital meter, blind-spot detection radar, and automotive data network.

Wei-Jen Chen was born in Taipei, Taiwan, R.O.C., in 1978. He received the B.S. and M.S. degrees in communication engineering from National Chiao Tung University, Hsinchu, Taiwan, R.O.C., in 2000 and 2002, respectively. He is currently engaged in the development of RF front-end module for GSM cell phones at Compal Communication Inc., Taipei, Taiwan, R.O.C.

Shyh-Jong Chung was born in Taipei, Taiwan, R.O.C. He received the B.S.E.E. and Ph.D. degrees from National Taiwan University, Taipei, Taiwan, R.O.C., in 1984 and 1988, respectively. Since 1988, he has been with the Department of Communication Engineering, National Chiao Tung University, Hsinchu, Taiwan, R.O.C., where he is currently a Professor. From September 1995 to August 1996, he was a Visiting Scholar with the Department of Electrical Engineering, Texas, A&M University, College Station. His areas of interest include the design and applications of active and passive planar antennas, communications in intelligent transportation systems (ITSs), LTCC-based RF components and modules, packaging effects of microwave circuits, and numerical techniques in electromagnetics. Dr. Chung received the Outstanding Electrical Engineering Professor Award of the Chinese Institute of Electrical Engineering and the Teaching Excellence Awards of National Chiao Tung University both at 2005. He served as the Treasurer of IEEE Taipei Section from 2001 to 2003 and the Chairman of IEEE MTT-S Taipei Chapter from 2005 to 2007.